

Dendromesogens: Liquid Crystal Organizations versus Starburst Structures

Joaquín Barberá, Mercedes Marcos, and José Luis Serrano*^[a]

Abstract: The synthesis and the liquid crystalline behavior of a novel series of poly(amidoamine) (PAMAM)-dendrimer derivatives is described. The series consists of five new compounds that contain 4, 8, 16, 32, and 64 peripheral mesogenic ester units attached to the 0-, 1-, 2-, 3-, and 4-generation of poly(amidoamine) (PAMAM), respectively. These five compounds exhibit a

smectic A mesophase, for which a structural model is proposed that is valid for several generations of dendrimers. This model is based on a structural character-

Keywords: dendrimers • dendromesogens • liquid crystals • structure elucidation • supramolecular chemistry

ization which mainly consists of X-ray diffraction studies. The molecules of these compounds exhibit a high degree of plasticity and tend to adopt the most convenient shape to afford liquid crystalline behavior. The mesogenic units form parallel aggregations that give rise to the smectic structure.

Introduction

As a class of new materials, dendrimers have, in recent years, generated a great deal of interest within the scientific community.^[1] One of the most attractive peculiarities of such compounds is the generation of macrostructures which show a regular structural growth, and such systems could exhibit new and interesting properties for use in new applications.^[2] Another important feature is the reactivity of the terminal groups into which we can introduce new moieties with specific functions; this makes it possible to modulate the properties of these dendrimer derivatives.^[3] Both approaches have been used to obtain dendrimers that show liquid crystalline arrangements (*dendromesogens* in the words of G. Lattermann).^[4] In this way Tomalia et al.^[5] in 1988, Ringsdorf et al.^[6] and, in particular, Percec et al.^[7] have reported several series of hyperbranched polymers based on flexible polyfunctionalized mesogens that exhibit nematic liquid crystalline behavior. This phenomenon arises from the ability of the molecules to fold into an anisotropic shape. Alternatively, other dendritic architectures that display liquid crystal properties include rodlike^[8] or disklike^[9] mesogenic groups in the periphery of the molecule which can form a liquid crystal shell around the central nucleus.

This paper deals with the latter type of dendromesogen and reports the synthesis and liquid crystalline properties of five new compounds derived from poly(amidoamine) (PAMAM)

dendrimers. For this purpose we have introduced 4, 8, 16, 32, and 64 terminal mesogenic ester units by attaching them to the 0-, 1-, 2-, 3-, and 4-generation of PAMAM, respectively. These changes tune the properties of the dendrimers (Scheme 1).

Typical PAMAM dendrimeric structures tend to adopt a globular structure in solution, especially when a large number of terminal units are involved (the formation of intramolecular H bonds could contribute to this phenomenon to a large extent).^[10] Interestingly, two driving forces compete in our compounds: the central PAMAM (polyamidoamine) starburst polymer leads to a spherical arrangement, while the mesogenic terminal units tend to interact with each other to form parallel aggregations that give rise to the liquid crystal state.

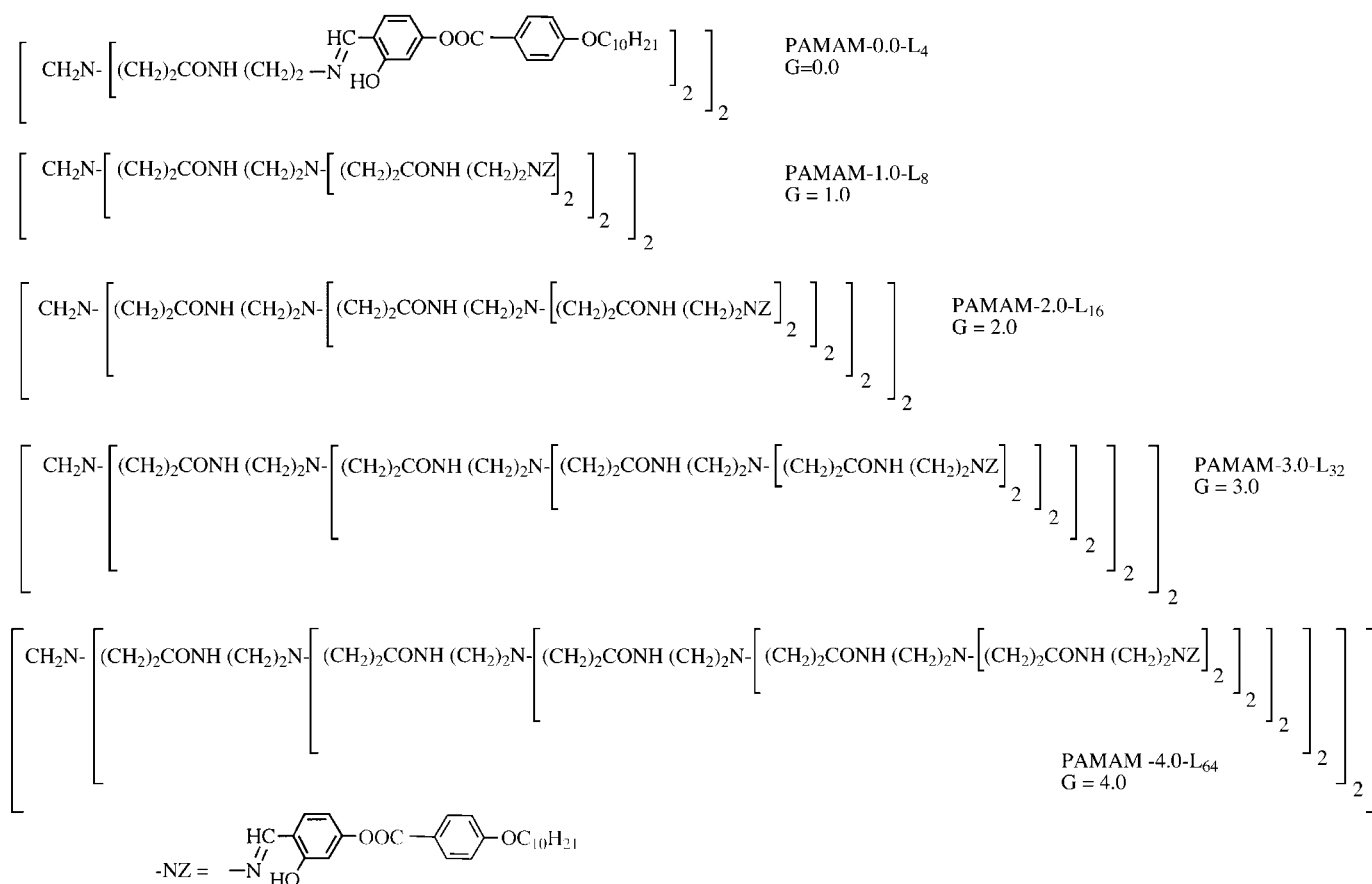
We have investigated the supramolecular liquid crystalline organization observed in these molecules. These investigations allow us to draw interesting conclusions about the molecular plasticity of this type of dendromesogen and even to predict the mesogenicity of new generations of homologous dendrimers or similar dendrimeric structures.

Results and Discussion

Synthesis: The dendrimers were synthesized by the condensation of 4-(4'-decyloxybenzoyloxy)salicylaldehyde with the terminal amino groups of the corresponding generation of PAMAM (0, 1, 2, 3, and 4) (Scheme 2).

All the compounds were isolated as air-stable yellow solids that are soluble in solvents such as dichloromethane, chloroform, and THF, and are insoluble in ethanol.

[a] Prof. J. L. Serrano, Dr. J. Barberá, Dr. M. Marcos
Química Orgánica, Facultad de Ciencias-ICMA,
Universidad de Zaragoza-CSIC, E-50009 Zaragoza (Spain)
Fax: (+34) 976-761209
E-mail: joseluis@posta.unizar.es



Scheme 1. Structures of the PAMAM dendrimers.

Characterization: The chemical structures of these compounds were established on the basis of ^1H NMR, ^{13}C NMR, and IR spectroscopy, FAB⁺ and MALDI-TOF mass spectrometry, gel permeation chromatography (GPC), and elemental analysis. All these techniques gave satisfactory results.

IR, ^1H NMR, and ^{13}C NMR spectroscopy have proved very useful in confirming the structure and the purity of these materials. Interestingly, the spectra of these materials closely resemble those of typical polyamides. Evidence for the condensation reactions was provided by the lack of a signal

at $\delta = 195$ in the ^{13}C NMR spectra (which corresponds to the carbonyl group of the aldehyde) along with the total absence of the NH_2 signals from the starting compound in the ^1H NMR and IR spectra. In addition, the excellent solubility of these dendrimers in CDCl_3 allowed us to integrate the different peaks in the ^1H NMR spectra, confirming in all cases that the expected polymer had been obtained.

The molecular masses of the higher molecular weight dendrimers (PAMAM-2.0-L₁₆, PAMAM-3.0-L₃₂, and PAMAM-4.0-L₆₄) could not be measured by either FAB⁺ or MALDI-TOF techniques. In contrast, the lower molecular weight dendrimers (PAMAM-0.0-L₄ and PAMAM-1.0-L₈) exhibit good FAB⁺ and MALDI-TOF spectra that contain peaks for the $[M^+]$ and $[M^++\text{Na}]$ ions. GPC measurements (mobile phase: THF; calibration standard: polystyrene) confirmed the presence of practically monodisperse polymers in all cases. However, as is often the case with dendrimers, a marked deviation from the calculated molecular weight was found in the experimental data, even for the low molecular weight compounds.^[11]

Mesogenic behavior: The liquid crystalline properties of these compounds were studied by polarizing optical microscopy, differential scanning calorimetry (DSC), and X-ray diffraction. The thermal and thermodynamic data are summarized in Table 1.

All the dendrimers exhibit liquid crystalline behavior. With the exception of compound PAMAM-1.0-L₈, the compounds

Abstract in Spanish: *Se describe la síntesis y el comportamiento como cristal líquido de una nueva serie de dendrímeros derivados de PAMAM. La serie consta de cinco nuevos compuestos que contienen 4, 8, 16, 32 y 64 unidades éster mesógenas periféricas enlazadas a la generación 0, 1, 2, 3 y 4 de poli(amidoamina) (PAMAM), respectivamente. Los cinco compuestos investigados presentan una mesofase esméctica A, para la que se propone un modelo estructural válido para varias generaciones de dendrímeros. Este modelo se basa en una caracterización estructural que consiste principalmente en estudios de rayos X. Las moléculas de estos compuestos muestran un alto grado de plasticidad y tienden a adoptar la forma más conveniente para proporcionar comportamiento de cristal líquido. Las unidades mesógenas forman agregados paralelos que dan lugar a la estructura esméctica.*

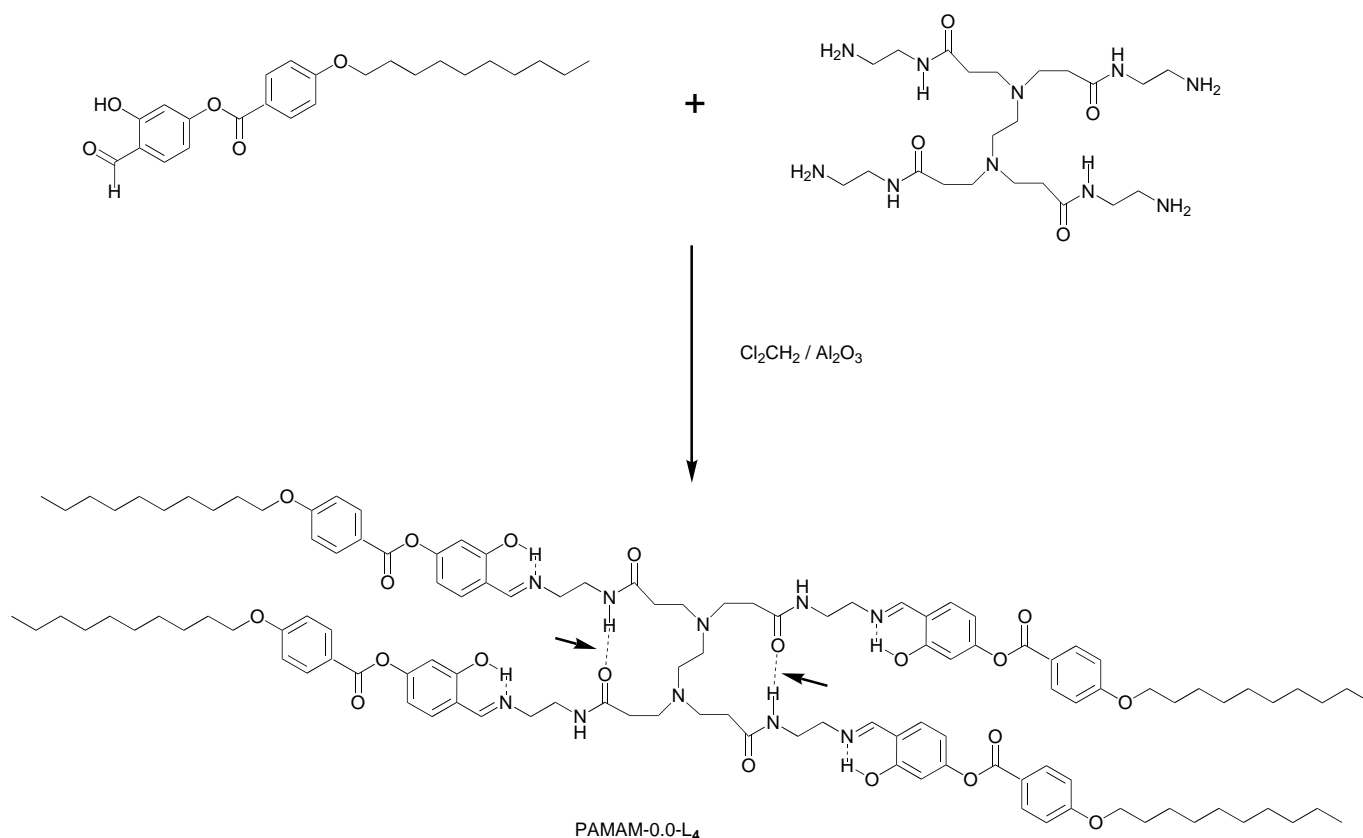
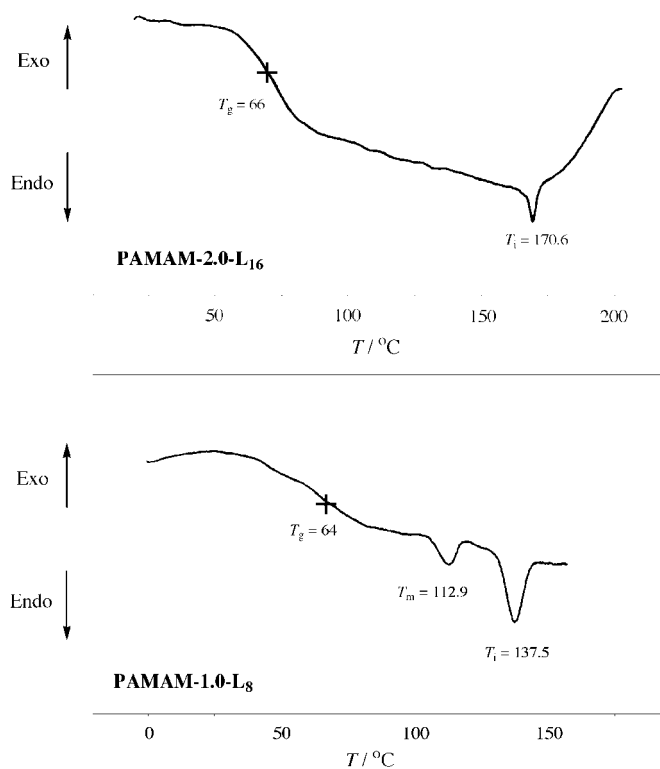
Scheme 2. Synthesis of PAMAM-0.0-L₄.

Table 1. Thermal and thermodynamic data of the phase transitions of the LC dendrimers.

LC dendrimer	Transition temperatures [°C] and ΔH in parentheses [J g ⁻¹]
PAMAM-0.0-L ₄	g 62 SmA 135.6 (8.6) I
PAMAM-1.0-L ₈	g 64 C 112.9 (1.0) SmA 137.5 (2.4) I
PAMAM-2.0-L ₁₆	g 66 SmA 170.6 (1.6) I
PAMAM-3.0-L ₃₂	g 65 SmA 184.8 (1.2) I
PAMAM-4.0-L ₆₄	g 67 SmA 181.7 (0.5) I

are obtained in an amorphous state and melt into a fluid mesophase at relatively low temperatures. The first heating scan did not afford easily identifiable textures. However, on cooling the isotropic liquid, small bâtonnets appeared which changed to give a homeotropic texture under mechanical stress. This behavior suggests a lamellar orthogonal mesophase; this was confirmed by X-ray measurements and identified as a smetic A mesophase (SmA).

These dendrimers behave as typical polymers and, in general, the DSC curves appear complex for the first heating scan. However, in the second scan after an annealing process, very simple thermograms were obtained and only the glass transition (T_g) and the isotropization transition (T_i) could be observed (see Table 1 and Figure 1 top).^[12] The only exception is compound PAMAM-1.0-L₈, which shows a melting transition (T_m) in both the first and the second heating scans in addition to the aforementioned transitions (Figure 1 bottom). The mesophases freeze at low temperature and it is not possible to observe the crystallization, even at -40°C .

Figure 1. DSC curves corresponding to the second heating scan (after an annealing process) of the compounds PAMAM-2.0-L₁₆ (top) and PAMAM-1.0-L₈ (bottom).

X-ray diffraction: The X-ray patterns are qualitatively similar in all cases.^[13] The patterns contain a set of two or three equally spaced sharp rings in the small-angle region, and a diffuse, broad halo in the wide-angle region (Figure 2a). The presence of the equally spaced maxima [reciprocal spacings in the ratio 1:2(:3)] is characteristic of a well-developed layer structure. The maxima correspond respectively to the first-, second-, and third-order reflections on the smectic planes, whereas the wide-angle halo indicates the existence of only short-range order (liquid-like order) within the layers. This kind of pattern is consistent with a smectic A mesophase. The measured distances are given in Table 2.

All the patterns are characteristic of un-oriented (powder) samples, as revealed by the presence of diffraction rings as opposed to arc or crescent-shaped spots. Aligned samples were obtained by stretching the samples against the capillary wall with a glass or metal rod at a temperature slightly lower than the clearing point.

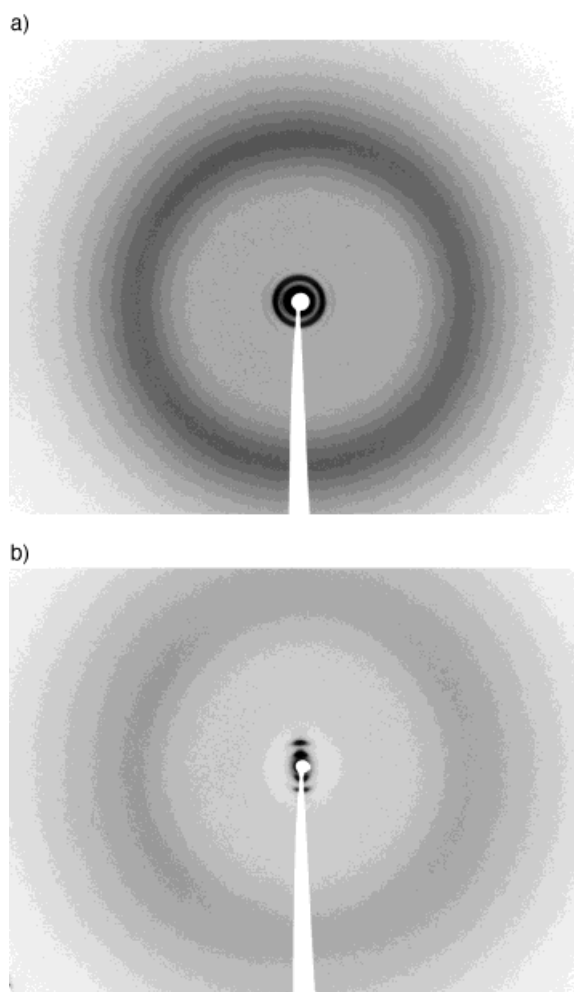


Figure 2. X-ray diffraction photographs of the frozen SmA mesophase of PAMAM-2.0-L₁₆ at room temperature: a) unoriented pattern and b) aligned pattern. The alignment direction is horizontal.

Table 2. X-ray data of the compounds.

Compound	Measured distances [Å]	<i>hkl</i>	Layer thickness <i>d</i> [Å]	Molecular area [(Å) ²]	Area per mesogenic unit [(Å) ²]
PAMAM-0.0-L ₄	51.9	0 0 1	52.0	65	32.5
	26.1	0 0 2			
	4.5(broad)				
PAMAM-1.0-L ₈	57.2	0 0 1	57.3	130	32.5
	28.7	0 0 2			
	4.4(broad)				
PAMAM-2.0-L ₁₆	59.3	0 0 1	59.5	261	32.6
	29.9	0 0 2			
	4.5(broad)				
PAMAM-3.0-L ₃₂	60.5	0 0 1	60.3	525	32.8
	30.2	0 0 2			
	20.0	0 0 3			
	4.5(broad)				
PAMAM-4.0-L ₆₄	61.1	0 0 1	61.0	1050	32.8
	30.5	0 0 2			
	20.3	0 0 3			
	4.5(broad)				

Oriented patterns were obtained when the samples submitted to this treatment were irradiated at room temperature. In the resulting patterns the small-angle maxima appear as a set of spots aligned along the direction perpendicular to the alignment direction, whereas the diffuse halo remains as an almost isotropic ring (Figure 2b). These features indicate that the smectic layers become oriented along the stretching direction (i. e. the stretching direction is contained in the smectic planes); however, the orientational order within the layers is poor.

Supramolecular organization in the mesophase: As can be seen from the results presented in Table 1, all the compounds show a SmA phase. However, as we explained above, a globular structure should be expected, at least for the materials of the highest generations which bear a large number of terminal units.^[10] Since a SmA phase is typical of elongated molecules, two questions arise: what is the preferred molecular conformation and what is the nature of the molecular packing in the mesophase?

As regards the first question, in principle two conformations could be possible in a general sense: a *radial* conformation or a *parallel* conformation (Figure 3). In the first case the mesogenic units are *radially* arranged around a central moiety to which they are linked by a variable number of amidoamine units that extend from that point (the molecules's center of mass). In the *parallel* model the flexible poly(amidoamine) chains would adopt the appropriate conformation to allow the mesogenic units to be parallel to each other, probably extending up and down from the molecule center.

In order to gain an insight into this point, some calculations can be made based on density estimations and the measured values of the layer thickness. The molecular volume can be estimated from the molecular mass and the density. The molecular area in Å² can then be expressed as $area = V/d$, where V is the molecular volume in Å³ and d is the layer thickness in Å. Table 2 lists the calculated molecular areas, assuming that the density of these compounds must be close to 1 g cm⁻³. Interestingly, the values obtained are directly proportional to the number of mesogenic units. This is

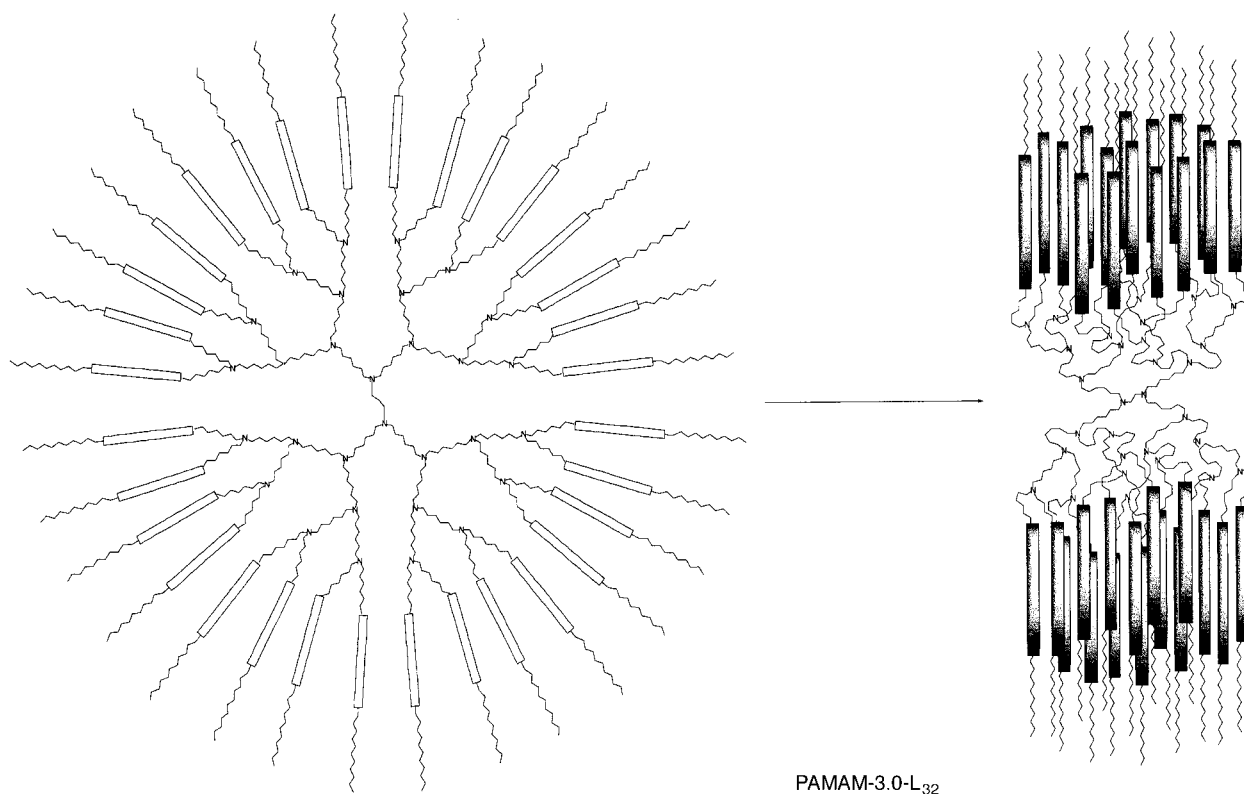


Figure 3. Schematic view of the two possible molecular conformations of the PAMAM dendromesogens. Left) *Radial* arrangement of the mesogenic units. Right) *Parallel* arrangement of the mesogenic units.

consistent with the *parallel* model. Table 2 also lists the area per mesogenic unit, with the assumption of an ideal structure in which half of the mesogenic units extend upwards and half of the mesogenic units extend downwards from the molecular center. An almost constant value of $32.5\text{--}32.8 \text{ \AA}^2$ was calculated in all cases. The proposed structural model is represented schematically in Figure 4. The poly(amidoamine) spacers are conformationally disordered and occupy the central slab of the smectic layers; the mesogenic units extend to both sides. The conformational disorder of the poly(amidoamine) groups (and of the peripheral decyloxy chains) explains the nearly isotropic character of the wide-angle halo, associated with the intralayer order, found in the aligned X-ray patterns.

Additional support for the proposed model comes from a graphical view of the evolution of the measured layer thickness, that should correspond to the molecular length, as the generation number increases (Figure 5). Although we assume a cylindrical model as the most simple structure, this simple molecular model will be deformed in the mesophase in order to fill the space between the neighboring molecules. The increase observed in the layer thickness from PAMAM-0.0-L₄ to PAMAM-1.0-L₈ is associated with a preferentially extended conformation of the amidoamine group. The increase in the molecular length is smaller from PAMAM-1.0-L₈ to PAMAM-2.0-L₁₆, and finally the increase is very small for the highest generation derivatives. For the latter, the poly(amidoamine) groups tend to fill all the space in the central part of the molecule, which means that they must adopt a very curled arrangement, and therefore

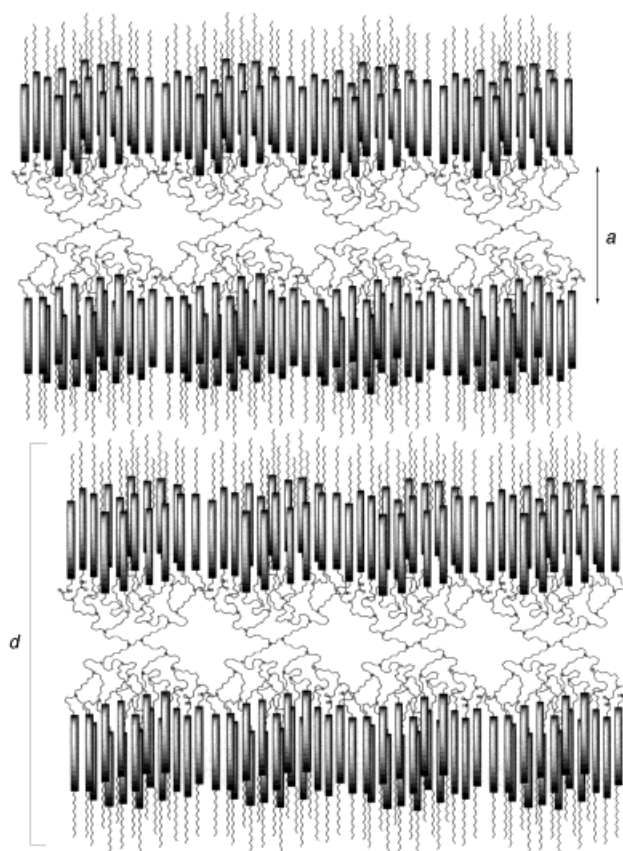


Figure 4. Schematic drawing of the proposed molecular packing of the PAMAM dendromesogens in the mesophase. *a* corresponds to the region occupied by the poly(amidoamine) spacers and *d* is the layer thickness.

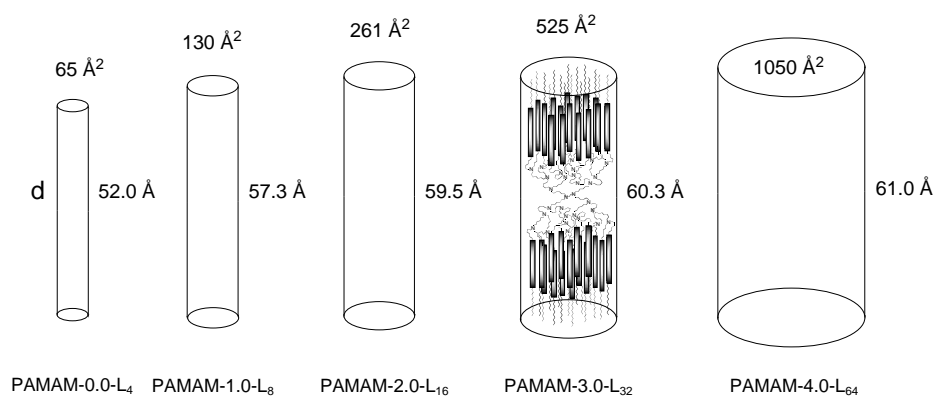


Figure 5. Evolution of the molecule size versus the generation number in PAMAM dendromesogens. The molecules are assumed to adopt an ideal cylindrical shape.

they contribute mainly to the molecular width rather than to the molecular length.

The formation of H bonds between the amido groups contributes to the maintenance of a stable aggregation of the central structure, which plays a special role in the behavior of the PAMAM central group. The existence of these hydrogen bonds has been proved by means of spectroscopic methods, mainly by IR and ¹H NMR spectroscopy.^[14]

On the basis of the parallel model, it could be possible to predict the molecular parameters of the hypothetical cylinder corresponding to further generations. A clear trend is observed for both the molecular length and the molecular width (measured as the diameter of the cylinder). Thus, for the sixth generation, the molecular diameter is expected to exceed the molecular length (Figure 6). However, if we consider the most extended structure of the PAMAM central core, corresponding to the all-*trans* conformation of the branches extended in the plane perpendicular to the molecular axis, it is possible to maintain the molecular model. For example, for the sixth generation the molecular diameter calculated by extrapolating the corresponding curve in Fig-

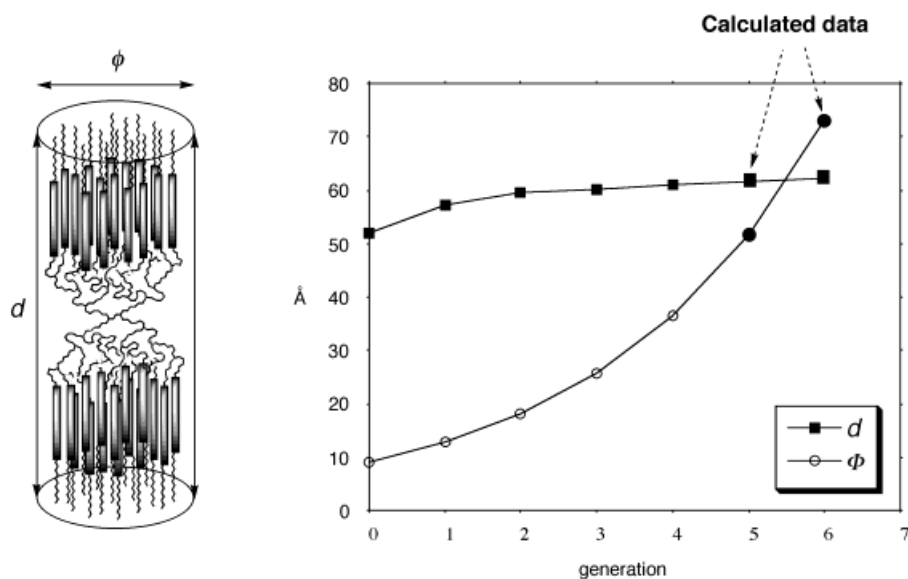


Figure 6. Graphical representation of the molecule length d and the molecule diameter ϕ versus the generation number in PAMAM dendromesogens. ϕ was estimated from the molecular areas in Table 2 and Figure 5 assuming an ideal circular section.

ure 6 is ≈ 73 Å, whereas the all-*trans* PAMAM central structure could extend up to ≈ 100 Å.

In addition to this, and taking into account that the liquid crystalline behavior depends mainly on the mesogenic cores, we can extend this type of calculation to other central dendrimeric structures that bear the same peripheral mesogenic units. Thus, preliminary studies with the poly(propylene imine) dendrimers (DAB-dendr)^[15] yield comparable results.^[16]

Another interesting possibility for these materials is the introduction of metals into two different parts of the molecule: into the coordination position of the imine-hydroxy groups of the mesogenic core in a similar manner to the classical salicylideneamine metallomesogenic complexes,^[17] or into the PAMAM central structure.^[18] Complexation with metals would be expected to modify the dendrimeric structure and consequently the liquid crystalline properties.

Experimental Section

Techniques: Microanalyses were performed with a Perkin-Elmer 240B microanalyzer. Infrared spectra were obtained with a Perkin-Elmer 1600 (FTIR) spectrophotometer in the range $\nu = 400\text{--}4000$ cm⁻¹. ¹H and ¹³C NMR spectra were recorded on a Varian Unity 300 MHz spectrometer in CDCl₃ solutions. Mass spectra were obtained with a VG Autospec spectrometer with positive-ion FAB (FAB⁺) (3-nitrobenzyl alcohol (NBA)). MALDI-TOF (matrix-assisted laser desorption/time-of-flight) mass spectra were obtained with a Kratos Analytical Kompact Maldi 2 K-Probe operating in a positive mode, and were analyzed by the associated

software on a Sun AparcStation 4. Samples were applied to the sample slides by first depositing the matrix dissolved in THF (10 mg mL⁻¹, 0.5 mL), followed by the sample dissolved in CH₂Cl₂ (≈ 1 mg mL⁻¹, 0.5 mL), and the slides were then air-dried. Gel permeation chromatography (GPC) was carried out in a Waters liquid chromatography system equipped with a 600E multisolvent delivery system and 996 photodiode array detector. Two Ultrastayage columns (Waters; pore size: 500 and 10⁴ Å) were connected in series. THF was used as the mobile phase with a flow rate of 0.8 mL min⁻¹. Calibration was performed with polystyrene standards. The optical textures of the mesophases were studied with a Meiji polarizing microscope equipped with a Mettler FP8 hot-stage and an FP80 central processor. The transition temperatures and enthalpies were measured by differential scanning calorimetry with a Perkin-Elmer DSC-7 instrument which was operated at a scanning

rate of $10^{\circ}\text{Cmin}^{-1}$ on heating. The apparatus was calibrated with indium (156.6°C ; 28.4 Jg^{-1}) as the standard. X-ray diffraction experiments were carried out on powder samples in a pinhole camera (Anton–Paar) operating with a Ni-filtered $\text{CuK}\alpha$ beam. The samples were held in Lindemann glass capillaries (1 mm diameter), and the X-ray patterns were collected on a flat photographic film.

General procedure for the condensation of 4-(4'-decyloxybenzoyloxy)salicylaldehyde with PAMAM dendrimers: To a stirred solution of 4-(4'-decyloxybenzoyloxy)salicylaldehyde in CH_2Cl_2 (15 mL) was added neutral activated grade I alumina (0.5 g) and then the corresponding poly(amido-amine). The mixture was refluxed under nitrogen until the aldehyde had completely reacted (usually 8–10 h). The alumina was filtered off and the solvent from the filtrate evaporated under vacuum. The resulting solid was dissolved in hexane and precipitated from ethanol. Yields: 70–85%.

Characterization: Because of the similarity of the ^1H and ^{13}C NMR spectra of these materials, we only quote the data for the PAMAM-2.0-L₁₆ dendrimer as a representative example. The data obtained from other techniques have been quoted for all compounds.

PAMAM-0.0-L₄: IR (Nujol): $\tilde{\nu} = 3295, 3068(\text{CON-H}), 1727(\text{OC=O}), 1656$ (sh, OC-NH), 16373 cm^{-1} (CH=N); elemental analysis calcd for $\text{C}_{118}\text{H}_{160}\text{N}_{10}\text{O}_{20}$ (%): C 69.54, H 7.85, N 6.87; found: C 69.9, H 7.3, N 6.6; FAB-MS (NBA matrix): m/z : 2061 $[\text{M}+\text{Na}]^+$; MALDI-TOF: m/z : 2038.7 $[\text{M}^+]$.

PAMAM-1.0-L₈: IR (Nujol): $\tilde{\nu} = 3277, 3083(\text{CON-H}), 1732(\text{OC=O}), 1656$ (sh, OC-NH), 1635 cm^{-1} (CH=N); elemental analysis calcd for $\text{C}_{254}\text{H}_{352}\text{N}_{26}\text{O}_{44}$ (%): C 68.21, H 7.87, N 8.14; found: C 68.0, H 7.8, N 8.0; FAB-MS (NBA matrix): m/z : 4475 $[\text{M}+1]^+$; MALDI-TOF: m/z : 4497.4 $[\text{M}+\text{Na}]^+$.

PAMAM-2.0-L₁₆: ^1H NMR (300 MHz, CDCl_3) $\delta = 13.7$ (s, 4H), 8.20 (s, 4H), 8.03(d, $J = 9$ Hz, 8H), 7.82 (brs, 4H), 7.13 (d, $J = 8$ Hz, 4H), 6.89 (d, $J = 9$ Hz, 8H), 6.64 (d, $J = 2$ Hz, 7H), 6.56 (dd, $J = 8$ Hz, $J = 2$ Hz, 4H), 3.97 (t, 8H), 3.70–3.55 (m, 7H), 3.55–3.40 (m, 8H), 3.25–3.10 (m, 8H), 2.75–2.55 (m, 14H), 2.55–2.40 (m, 6H), 2.40–2.20 (m, 14H), 1.85–1.70 (t, 8H), 1.50–1.20 (m, ≈ 56 H), 0.85 (t, $J = 7$ Hz, 12H); ^{13}C NMR (300 MHz, CDCl_3) $\delta = 173.16, 172.73, 165.78, 164.52, 164.25, 163.66, 154.61, 132.75, 132.31, 131.53, 121.06, 116.19, 114.32, 112.07, 110.74, 68.33, 57.20, 50.0, 39.97, 33.94, 31.87, 29.54, 29.37, 29.30, 29.08, 25.96, 22.65, 14.10$; IR (Nujol): $\tilde{\nu} = 3306, 3069(\text{CON-H}), 1730(\text{OC=O}), 1659$ (sh, OC-NH), 1639 cm^{-1} (CH=N); elemental analysis calcd for $\text{C}_{526}\text{H}_{736}\text{N}_{58}\text{O}_{92}$ (%): C 67.63, H 7.88, N 8.70; found: C 67.3, H 7.5, N 8.7.

PAMAM-3.0-L₃₂: IR (Nujol): $\tilde{\nu} = 3314, 3100(\text{CON-H}), 1730(\text{OC=O}), 1658$ (sh, OC-NH), 1637 cm^{-1} (CH=N); elemental analysis calcd for $\text{C}_{1070}\text{H}_{1504}\text{N}_{122}\text{O}_{188}$ (%): C 67.37, H 7.88, N 8.96; found: C 67.4, H 8.1, N 8.9.

PAMAM-4.0-L₆₄: IR (Nujol): $\tilde{\nu} = 3306, 3069(\text{CON-H}), 1730(\text{OC=O}), 1656$ (sh, OC-NH), 1637 cm^{-1} (CH=N); elemental analysis calcd for $\text{C}_{2158}\text{H}_{3040}\text{N}_{250}\text{O}_{380}$ (%): C 67.23, H 7.89, N 9.08; found: C 66.9, H 7.8, N 9.0.

Acknowledgments

This work was supported by the Comisión Interministerial de Ciencia y Tecnología (Projects MAT97-0986-CO2-01 and MAT96-1073-CO2-02). The authors are grateful to Dr. D. Amabilino and Prof. J. Veciana (from Instituto de Ciencia de Materiales de Barcelona) for the MALDI-TOF mass spectra.

- [1] a) G. R. Newcome, C. N. Moorefield, F. Vögtle, *Dendritic Molecules: Concepts, Synthesis and Perspectives*, VCH, Weinheim, **1996**; b) D. A. Tomalia, A. M. Naylor, W. A. Goddard, III, *Angew. Chem.* **1990**, *102*, 118–157; *Angew. Chem. Int. Ed. Engl.* **1990**, *29*, 138–175.
- [2] a) O. A. Matthews, A. N. Shipway, J. F. Stoddart, *Prog. Polym. Sci.* **1998**, *23*, 1–56; b) Ref. [1a], pp. 241–250.
- [3] P. R. Ashton, S. E. Boyd, C. L. Brown, S. A. Nepogodiev, E. W. Meijer, H. W. I. Peerlings, J. F. Stoddart, *Chem. Eur. J.* **1997**, *3*, 974–984.
- [4] J. H. Cameron, A. Facher, G. Latterman, S. Diele, *Adv. Mater.* **1997**, *9*, 398–403.
- [5] S. E. Friberg, M. Podzimek, D. A. Tomalia, D. M. Hedstrand, *Mol. Cryst. Liq. Cryst.* **1988**, *164*, 157–165.
- [6] S. Bauer, H. Fischer, H. Ringsdorf, *Angew. Chem.* **1993**, *105*, 1658–1660; *Angew. Chem. Int. Ed. Engl.* **1993**, *32*, 1589–1592.
- [7] a) V. Percec, M. Kawasumi, *Macromolecules* **1992**, *25*, 3843–3850; b) V. Percec, P. Chu, M. Kawasumi, *Macromolecules* **1994**, *27*, 4441–4453; c) V. Percec, P. Chu, G. Ungar, J. Zhou, *J. Am. Chem. Soc.* **1995**, *117*, 11 441–11 454; d) V. S. K. Balagurusamy, G. Ungar, V. Percec, G. Johansson, *J. Am. Chem. Soc.* **1997**, *119*, 1539–1777; e) S. D. Hudson, H. T. Jung, V. Percec, W. D. Cho, G. Johansson, G. Ungar, U. S. K. Balagurusamy, *Science* **1997**, *278*, 449–452.
- [8] a) S. A. Ponomarenko, E. A. Rebrov, A. Y. Bobronsky, N. I. Boiko, A. M. Mugafarov, V. P. Shibaev, *Liq. Cryst.* **1996**, *21*, 1–12; b) K. Lorenz, D. Hölter, R. Mühlhaupt, H. Frey, *Adv. Mater.* **1996**, *8*, 414–416.
- [9] a) D. J. Pesak, J. S. Moore, *Angew. Chem.* **1997**, *109*, 1709–1712; *Angew. Chem. Int. Ed. Engl.* **1997**, *36*, 1636–1639; b) H. Meier, M. Lehmann, *Angew. Chem.* **1998**, *110*, 666–669; *Angew. Chem. Int. Ed.* **1998**, *37*, 643–645.
- [10] Y. Gao, K. H. Langley, F. E. Karasz, *Macromolecules* **1992**, *25*, 4902–4904.
- [11] P. L. Dubin, S. L. Edwards, J.-L. Kaplan, M. S. Mehta, D. A. Tomalia, J. Xia, *Anal. Chem.* **1992**, *64*, 2344.
- [12] The samples were submitted to an isothermal treatment for 2 hours at a temperature 50°C below the isotropic transition and then cooled to -40°C and heated at a rate of $10^{\circ}\text{Cmin}^{-1}$.
- [13] For this study the samples were loaded into Lindemann glass capillaries, heated to the isotropic liquid, and then cooled to room temperature. The frozen mesophases obtained in this way were irradiated for several hours.
- [14] The bands corresponding to associated amides are clearly detected in the IR spectra. The NH bond yields two bands similar to those observed for typical polyamides at $\nu \approx 3300\text{ cm}^{-1}$ (strong) and 3080 cm^{-1} (medium). The C=O bond of the amide group appears associated as a shoulder in the C=N imine band at $\nu \approx 1660\text{ cm}^{-1}$. The amide protons are detected by ^1H NMR spectroscopy as a broad peak between $\delta = 7.6$ and 7.9 .
- [15] E. M. M. de Brabander-van den Berg, E. W. Meijer, *Angew. Chem.* **1993**, *105*, 1370–1372; *Angew. Chem. Int. Ed. Engl.* **1993**, *32*, 1308–1311.
- [16] J. Barberá, M. Marcos, P. J. Alonso, J. I. Martínez, J. L. Serrano, 17th International Liquid Crystal Conference, **1998**, Strasbourg (France).
- [17] J. L. Serrano, T. Sierra in *Metalloenesogens. Synthesis, Properties and Applications* (Ed.: J. L. Serrano) VCH, Weinheim, **1996**; pp. 54–71.
- [18] M. F. Ottaviani, F. Montalti, N. J. Turro, D. A. Tomalia, *J. Phys. Chem. B* **1997**, *101*, 158–156.

Received: December 28, 1998 [F 1509]